ARTICLE

https://doi.org/10.1590/2317-4889202420240017

BJGEO Brazilian Journal of Geology

Unveiling the sedimentary infill of the Uruguayan onshore portion of the Pelotas Basin (southeast of Uruguay)

Ethel Morales[1,2*], Gerardo Veroslavsky[1,2], Rodrigo Umpierrez[1], Josefina Marmisolle[3], Facundo Plenc[1,2], Bruno Conti[3]

Abstract

The Uruguayan onshore portion of the Pelotas Basin is the Laguna Merin Basin. Despite its interesting geological and geophysical features, such as the highest Bouguer gravity anomaly and the youngest volcanic calderas in the country, it is the least known basin in Uruguay. In this study, a stratigraphic chart is presented for the first time, and an integrated analysis of its sedimentary infill is performed through the acquisition of horizontal-to-vertical spectral ratio data as well as geological and geophysical data available from previous studies. The Cretaceous sedimentary infill was restricted to the rift phase, corresponding to alluvial and fluvial deposits. The Cenozoic sedimentary cover corresponds to continental to marine sedimentary rocks and sediments deposited from the Oligocene to the present day in a drift tectonic framework. It presents a regional areal extension that exceeds the structural rifting borders of the basin. The maximum Cretaceous/Cenozoic sedimentary infill thickness is ~500 m. Cretaceous sedimentary units related to the rift and Oligocene drift phases are only present in the Uruguayan portion of the onshore Pelotas Basin, and the thickness of the Cenozoic drift deposits (from the Miocene to modern deposits) in the Brazilian region is at least twice that in the Uruguayan region.

KEYWORDS: HVSR; rift and drift sedimentation; Laguna Merín Basin.

1 INTRODUCTION

The Pelotas Basin, located between the Florianopolis High (border with the Santos Basin offshore of Brazil) and the Polonio High (border with the Punta del Este Basin offshore of Uruguay), occupies onshore and offshore areas of southeastern Brazil and Uruguay. It can be divided into two subbasins, North and South, separated by the Porto Alegre Lineament, which constitutes a structural feature that continues offshore (Porto Alegre Fracture Zone) (Bueno, 2021; Martins Neto et al., 2006) (Fig. 1).

The Uruguayan onshore portion of the Pelotas Basin is locally known as the Laguna Merín Basin (LMB; Bossi, 1966) (Fig. 1). Its genesis is related to the breakup of Western Gondwana and the later opening of the South Atlantic Ocean during the Late Jurassic-Early Cretaceous (Morales et al., 2022; Rossello et al., 1999; Sprechmann et al., 1981), and it has been controlled by large crustal discontinuities (NNE-NE) formed during the Brazilian Cycle (Chang et al., 1992; Machado et al., 2021). The structural rifting borders of the basin are represented to the north by the Cebollatí-Merín Lineament (CML) and to the south by the Aiguá-India Muerta-Chuy Lineament (AICL). The CML controls the NE inflection of the Merín Lagoon along the border Uruguay–Brazil and continues into Brazilian territory, controlling the development of the Patos Lagoon (Pelotas lineament; Rosa et al., 2009; Saadi, 1993; Saadi et al., 2002). In contrast, the AICL extends into the offshore (Chuy lineament; Bueno, 2021; Morales et al., 2022; Rosa et al., 2009) (Fig. 1).

The LMB has low relief with wetlands, flat topography, and scarce outcrops. In this large region, three landscape units have been recognized: *sierras*, small hills and hillock ridges, terraces, and fluvial plains (Achkar et al., 2012). High-relief areas are relegated to the structural borders of the basin where basement rocks outcrop or are located at very shallow depths and scarce areas where extrusive and subvolcanic acid igneous rock outcrop (Achkar et al., 2012; Panario, 1988).

Although the LMB presents interesting geological and geophysical features, such as the highest Bouguer gravity anomaly (Ellis & Turner, 2006; Reitmayr, 2001) and the youngest volcanic calderas (Cernuschi et al., 2015; Muzio et al., 2009; Rossello et al., 1999), it is the least known basin in the country. No wells have reached the crystalline Precambrian basement except at its

Supplementary material

Supplementary data associated with this article can be found in: https://doi.org/10.48331/scielodata.OUUPQ4.

[1]Universidad de la República, Facultad de Ciencias – Montevideo, Uruguay. E-mails: ethel@fcien.edu.uy, gerardo@fcien.edu.uy, rodrigo_u_17@hotmail.com, fplenc@fcien.edu.uy

[2]Programa de Desarrollo de las Ciencias Básicas – Montevideo, Uruguay.

[3]ANCAP – Montevideo, Uruguay. E-mails: jmarmisoll@ancap.com.uy, bconti@ancap.com.uy

*Corresponding author.

basin border; therefore, its depth, geometry, and infill remain unknown (Morales et al., 2022; Veroslavsky et al., 2004).

According to current knowledge, the igneous-sedimentary infill of the LMB comprises Cretaceous-Cenozoic sedimentary deposits located on top of thick Jurassic-Cretaceous igneous rocks (up to 2,500 m-thick), which are probably interbedded with sedimentary and/or volcanoclastic rocks in its lower half. Sedimentary cover and acidic to basic igneous complex rocks (including flows, sills, dykes, and calderas) have been identified in outcrops along the basin borders and wells (Bossi, 1966; Cernuschi et al., 2015; Morales et al., 2022; Muzio et al., 2009; Veroslavsky et al., 2004).

This study aims to characterize the sedimentary infill of the LMB through the acquisition of horizontal-to-vertical spectral ratio (HVSR) data, its integration with geological data from stratigraphic and groundwater wells, and geophysical data (magnetotelluric and long-range vertical electrical soundings) available from previous studies. The HVSR method is a non-invasive technique that uses a broadband, three-component seismometer that registers ambient seismic noise. It can be used in an effective way to estimate the depth and thickness of different geological units when there is a significant acoustic impedance contrast between them, for example, at the contact between sedimentary rocks and igneous rocks (Agostini et al., 2015; Lane et al., 2008), as such is the case of the LMB.

2 GEOLOGICAL SETTING

Uruguayan geology consists of a Precambrian Shield that includes Archean to Proterozoic rocks, outcropping mainly in the country's southern region, and three Phanerozoic sedimentary basins named Norte, Santa Lucía, and Laguna Merín (Fig. 1).

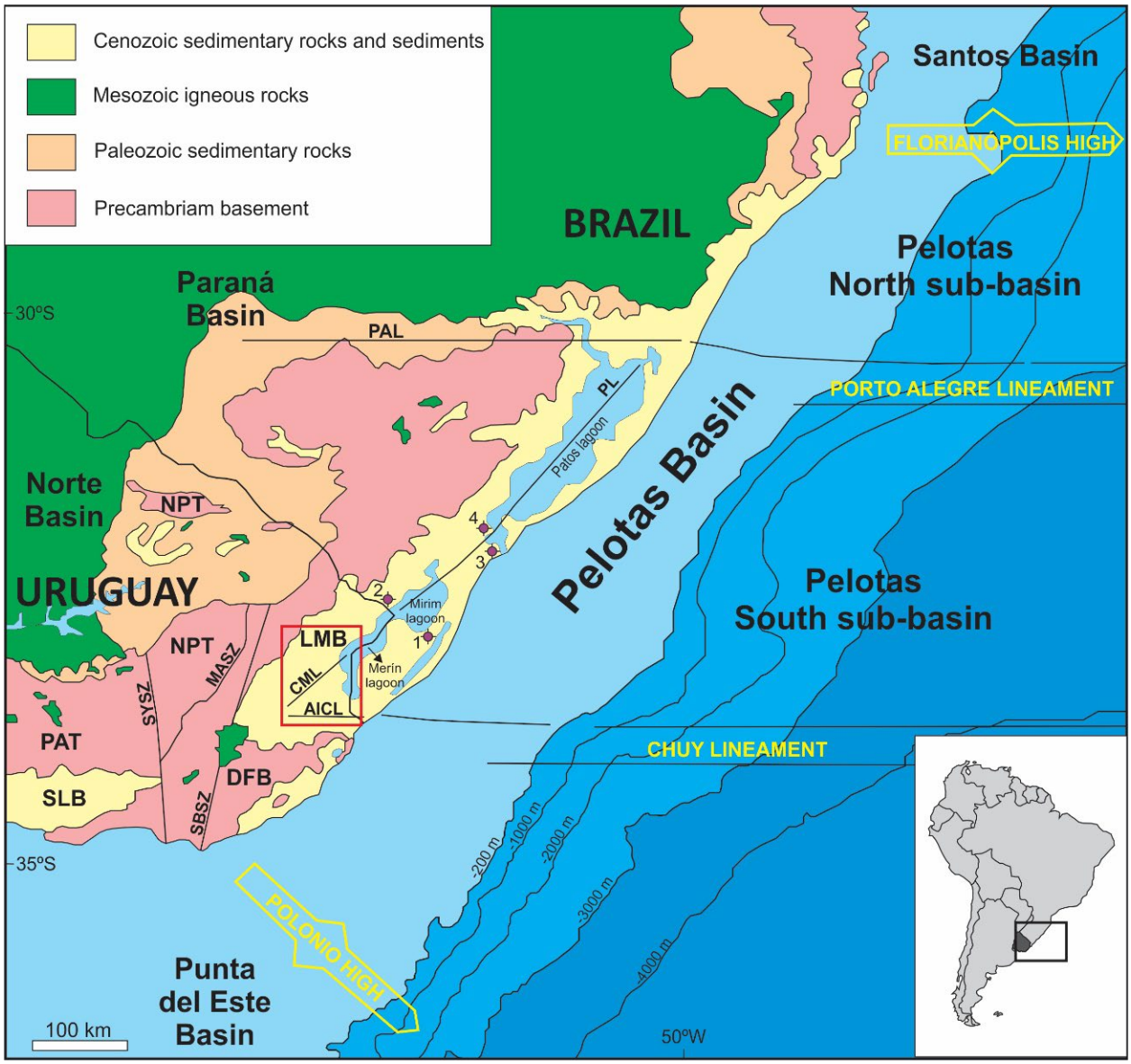

SYSZ: Sarandí del Yi Shear Zone; SBSZ: Sierra Ballena Shear Zone; MASZ: Mal Abrigo Shear Zone; PAL: Porto Alegre Lineament; AICL: Aiguá-India Muerta-Chuy Lineament; CML: Cebollatí-Merin Lineament; PL: Pelotas Lineament; DFB: Dom Feliciano Belt; NPT: Nico Pérez Terrane; PAT: Piedra Alta Terrane; SLB: Santa Lucía Basin; LMB: Laguna Merín Basin.

Figure 1. Simplified geological map of the southeast of Uruguay and Brazil (modified from Bossi et al., 2001; Rosa et al., 2009; Saadi et al., 2002). The red rectangle indicates the studied area. The location of the wells in the Brazilian territory mentioned in this work is indicated: 1: 2-CA-1-RS; 2: 2-PJ-1-RS; 3: 2-CI-1-RS; 4: 2PN-1-RS.

The Precambrian Shield consists of a collage of metamorphic and igneous rocks as well as various hypabyssal dyke swarms. Although its division into several tectonostratigraphic terranes is still a matter of debate, in general, it can be divided into the following three main domains (Fig. 1):

- the Piedra Alta terrane, which includes Paleoproterozoic rocks that were not tectonically reworked during the Neoproterozoic (Bossi et al., 2001; Oyhantçabal et al., 2011);
- the Nico Pérez terrane, consisting of Archean and Paleoproterozoic rocks tectonically reworked during the Neoproterozoic (Bossi et al., 2001; Oyhantçabal et al., 2011);
- the Dom Feliciano belt, representing the Brasiliano/Pan-African orogenic cycle (Bossi & Gaucher, 2004; Masquelin, 2006; Sánchez-Bettucci et al., 2021).

The DFB constitutes the basement of the LMB and is represented by three outstanding constituents: the Lavalleja Metamorphic Complex, the Punta Rasa-Campanero Complex, and the Sierra Ballena Shear Zone (Masquelin, 2006). A tectonic high in the DFB lies between the Uruguayan onshore and offshore portions of the Pelotas Basin (Goscombe et al., 2003).

The Norte Basin (the name given to the Uruguayan portion of the Paraná Basin) comprises Paleozoic to Mesozoic sedimentary rocks and Mesozoic basaltic flows mainly related to the evolution of Western Gondwana. Its infill is composed of four volcano-sedimentary megasequences: Devonian, Late Carboniferous–Permian, Jurassic–Cretaceous, and Late Cretaceous, separated by regional unconformities (de Santa Ana et al., 2006).

The Santa Lucía and Laguna Merín basins constitute rift structures that developed during the Late Jurassic–Early Cretaceous (Morales et al., 2022; Nuñez Demarco et al., 2020; Rossello et al., 1999; Veroslavsky et al., 2004). Rossello et al. (1999, 2000) state that both basins constitute the Santa Lucía–Aiguá–Merín (SaLAM), an E-NE extensive – dextral strike-slip structural corridor.

The LMB is limited to the west by the N-S trending SBSZ, north by the N60° CML, and south by the N85° AICL (Fig. 1) (Morales et al., 2022; Nuñez Demarco et al., 2020; Rossello et al., 1999, 2000; Veroslavsky et al., 2004). These structures controlled the main area of crustal extension and magmatic activity during the Jurassic–Early Cretaceous in southeastern Uruguay. However, north of the CML, a set of regional structures (e.g., Otazo Shear Zone, see Gómez-Rifas, 1995) and some magmatic relicts (e.g., Yaguarón dacites, see Bossi, 1966; Vieira, 1985) associated with the rift phase provide evidence that the geological units related to the initial rifting had a greater extension than currently preserved. Likewise, in the offshore portion of the basin, the rift phase magmatism is represented mainly by more than 2,000 m thick of several wedges of seaward dipping reflectors (SDR) (Chauvet et al., 2021; Morales et al., 2017; Soto et al., 2011).

Figure 2 presents the first stratigraphic chart of LMB developed from the literature and the results achieved in this study. The rift phase is represented mainly by igneous rocks throughout the basin, such as the Puerto Gómez Formation and secondarily by the Arequita Formation. The Puerto Gómez Formation (Bossi, 1966) comprises Jurassic to Early Cretaceous basic igneous rocks, predominantly basalts, and subordinate andesites, with a maximum drilled thickness of 1,138 m (Puerto Gómez well, Figs. 3 and 4). The Arequita Formation (Bossi, 1966) corresponds to Lower Cretaceous acidic igneous rocks, prominent rhyolites, and subordinate dacites, trachytes, and pyroclastic rocks (Muzio et al., 2009). The remaining igneous units have a restricted areal extension in the basin and constitute mainly high topographic areas, such as the subcircular alkaline *Macizo Valle Chico* complex, located at the west extreme of the basin (Muzio, 2000) and San Miguel Hill, located at the east extreme of the basin (Muzio et al., 2009). The rifting sedimentary infill is represented by the Migues Formation (Bossi, 1966), corresponding to Lower Cretaceous continental sandstones with minor levels of conglomerates and shales and a maximum drilled thickness of 64 m (Puerto Gómez well) (Veroslavsky et al., 2004; Vivanco et al., 2020).

The Cenozoic sedimentary cover (Oligocene to present, drift phase) presents a regional areal extension that exceeds the structural rifting borders of the basin (CML and AICL). It includes the Fray Bentos, Camacho, Paso del Puerto, Libertad, Chuy, Dolores, Villa Soriano formations, and modern sediments. The Fray Bentos Formation consists mainly of continental fine-grained sandstones and loess (Bossi, 1966; Ubilla, 2004). The marine Camacho Formation consists of fine-grained sandstones, claystones, and coquinas (Goso, 1985; Perea & Martínez 2004; Preciozzi et al., 1985). The Paso del Puerto Formation has a continental origin and consists mainly of interbedded sandstones, conglomerates, and shales (Bossi & Navarro, 1991; Preciozzi et al., 1985). The Libertad (continental) and Chuy (marine) formations represent several Pleistocene transgressive-regressive cycles (Goso, 1972, 1985; Martínez & Ubilla, 2004; Rojas, 2007). The Dolores formation is characterized by continental clay-silt and silt-clay deposits with interbedded sands and gravels (Goso, 1985; Martínez & Ubilla, 2004). The marine Villa Soriano Formation includes deposits ranging from clays to medium sands and subordinate gravels (Preciozzi et al., 1985; Ubilla & Martínez, 2016). Modern sediments are associated with alluvial, fluvial, and coastal lagoon systems.

3 MATERIALS AND METHODS

To characterize the sedimentary cover and determine its thickness in the study area, all available data from previous studies were collected, reviewed, and integrated into the analysis (Bossi, 1966; Cernuschi et al., 2015; Medina & Pirelli, 1995; Morales et al., 2022; Preciozzi et al., 1985; PRENADER 1993; Umpiérrez, 2022; Veroslavsky et al., 2004; Vivanco et al., 2020). Wells located onshore in the Brazilian portion of the basin, close to the border with Uruguay, were also included in this study (Rosa et al., 2009; Sanguinetti, 1980). Additionally, the HVSR method was applied mainly in the western sector of the basin, where available data are scarce and mostly consist of shallow groundwater wells (Fig. 3).

The HVSR method allows one to quickly determine the fundamental resonance frequency of a "soft" shallow layer (constituted by sediments or sedimentary rocks) that overlays

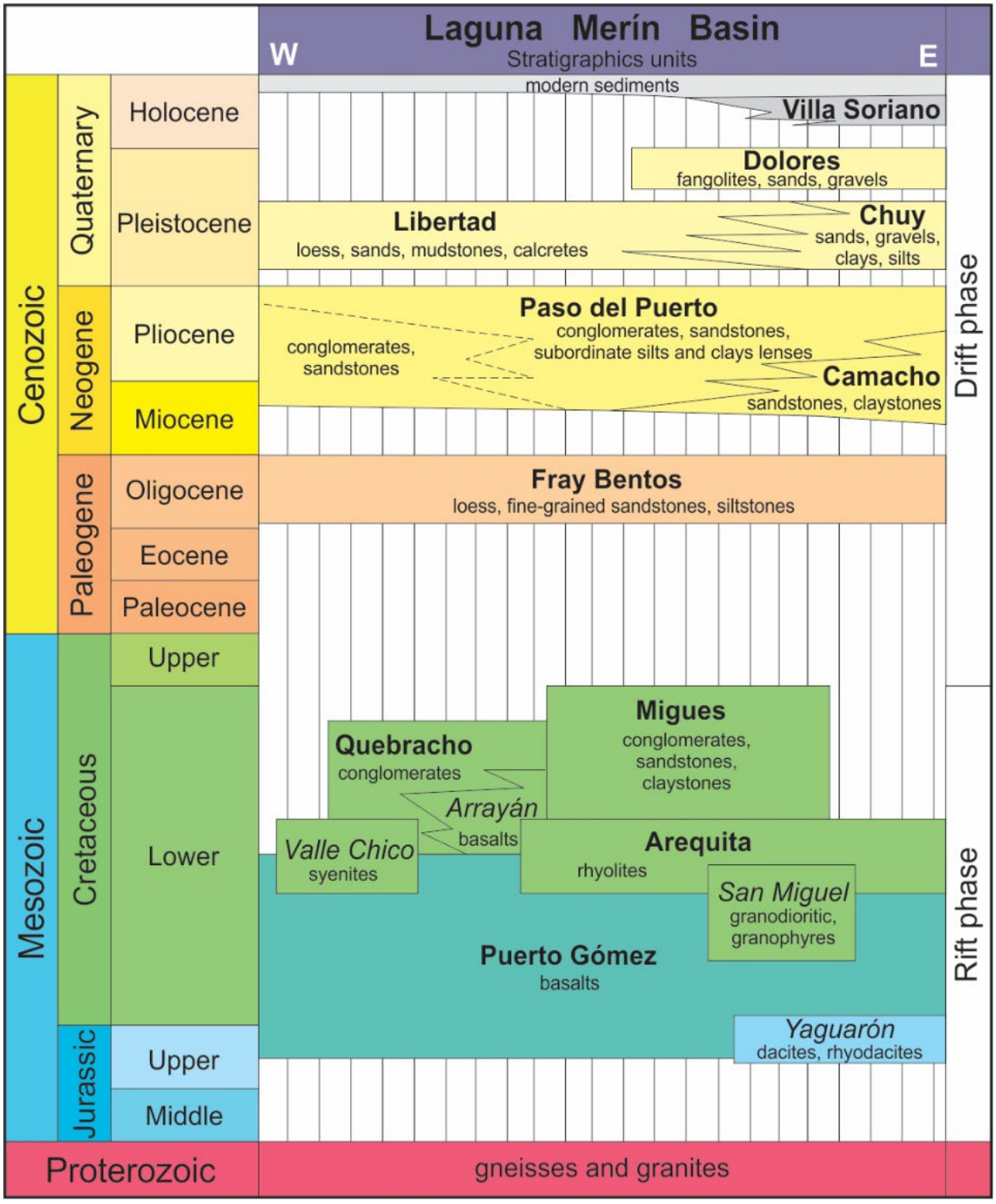

Figure 2. Stratigraphic chart of the LMB, including formal (bold) and unformal (italic) units.

a "hard" layer corresponding to the basement or its infill of the basin (e.g., basalts) in a range between 0 and more than 500 m (Lane et al., 2008; Owers et al., 2016). This method is a passive seismic technique that uses a three-component seismometer to measure the vertical and horizontal components (N-S, E-W) of ambient seismic noise generated by natural (e.g., oceanic waves, winds) or artificial processes (machinery and traffic) (Bard, 1998).

In total, 58 HVSR stations were measured (Fig. 3; complementary data) in the LMB. The recording time of each measurement (between 24 and 40 minutes) and a frequency range (between 0.1 and 256 Hz) were defined according to the local geology and the recommendations and guidelines provided by SESAME (Site EffectS assessment using AMbient Excitations 2004).

Grilla software was used to convert the three vibration components generated by ambient noise from time to the frequency domain and to visualize the combination of the spectral amplitudes of the horizontal (H) and vertical (V) components through H/V curves with distinct peaks. The different H/V

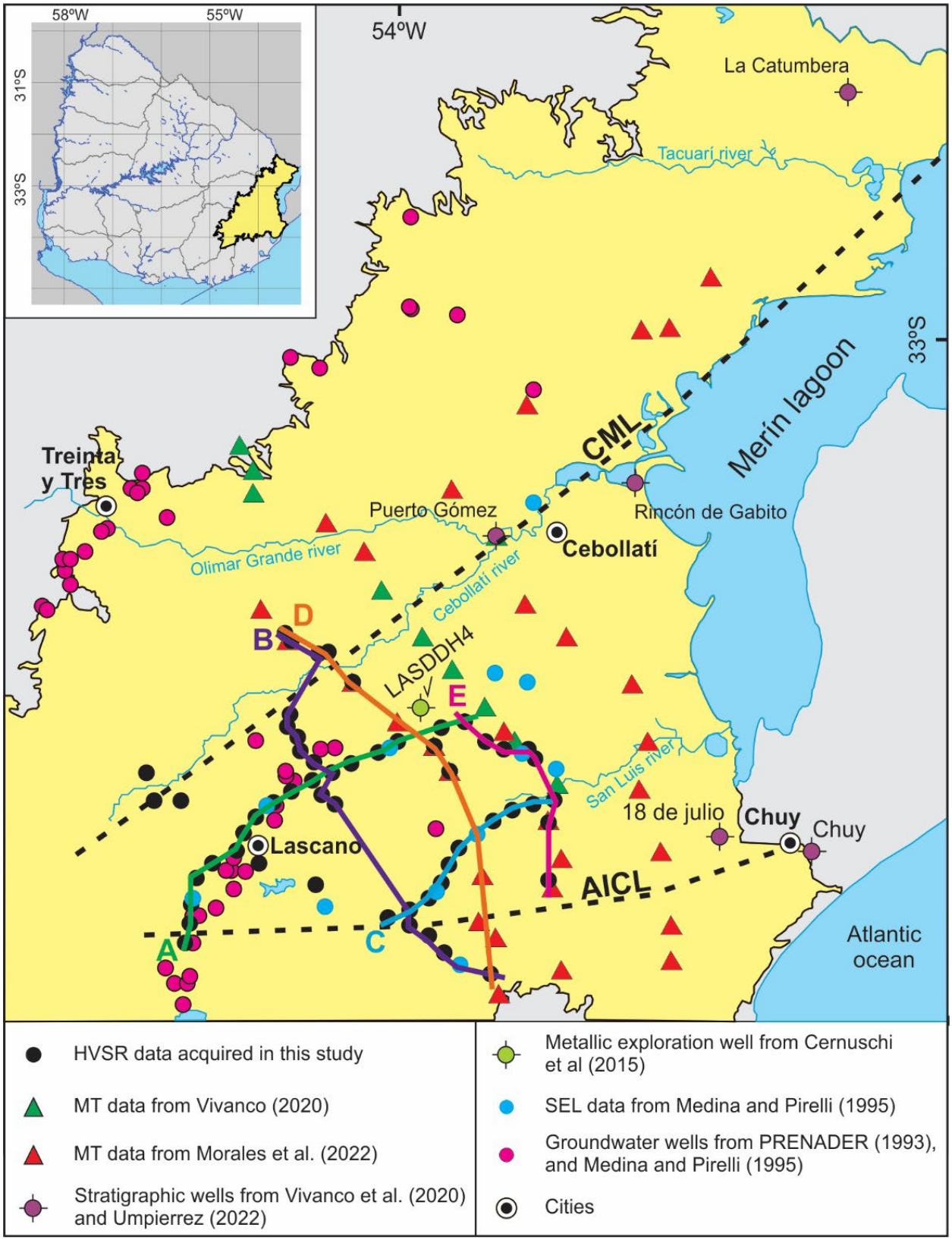

Figure 3. Database used in this study. AICL, Aiguá-India Muerta-Chuy Lineament; CML, Cebollatí-Merin Lineament. The (A–E) HVSR transect locations are indicated.

curves acquired along a section are displayed as contour graphics, in which the same color shades indicate equal H/V ratio amplitudes for generating 2D transects. The criteria for interpreting the reliability and geological significance of the H/V curves and their peaks are based on the SESAME (SESAME European Research Project, 2004) guide. Also, all the obtained H/V curves fulfilled the SESAME guide (SESAME European Research Project, 2004) criteria of "reliable curve," and the criteria for "clear peak" is met for most cases.

A total of 15 stratigraphic or metallic mineral exploration wells (total depth exceeding 100 m) were drilled into the LMB. Of these wells, five are referred to as "vintage" wells, drilled

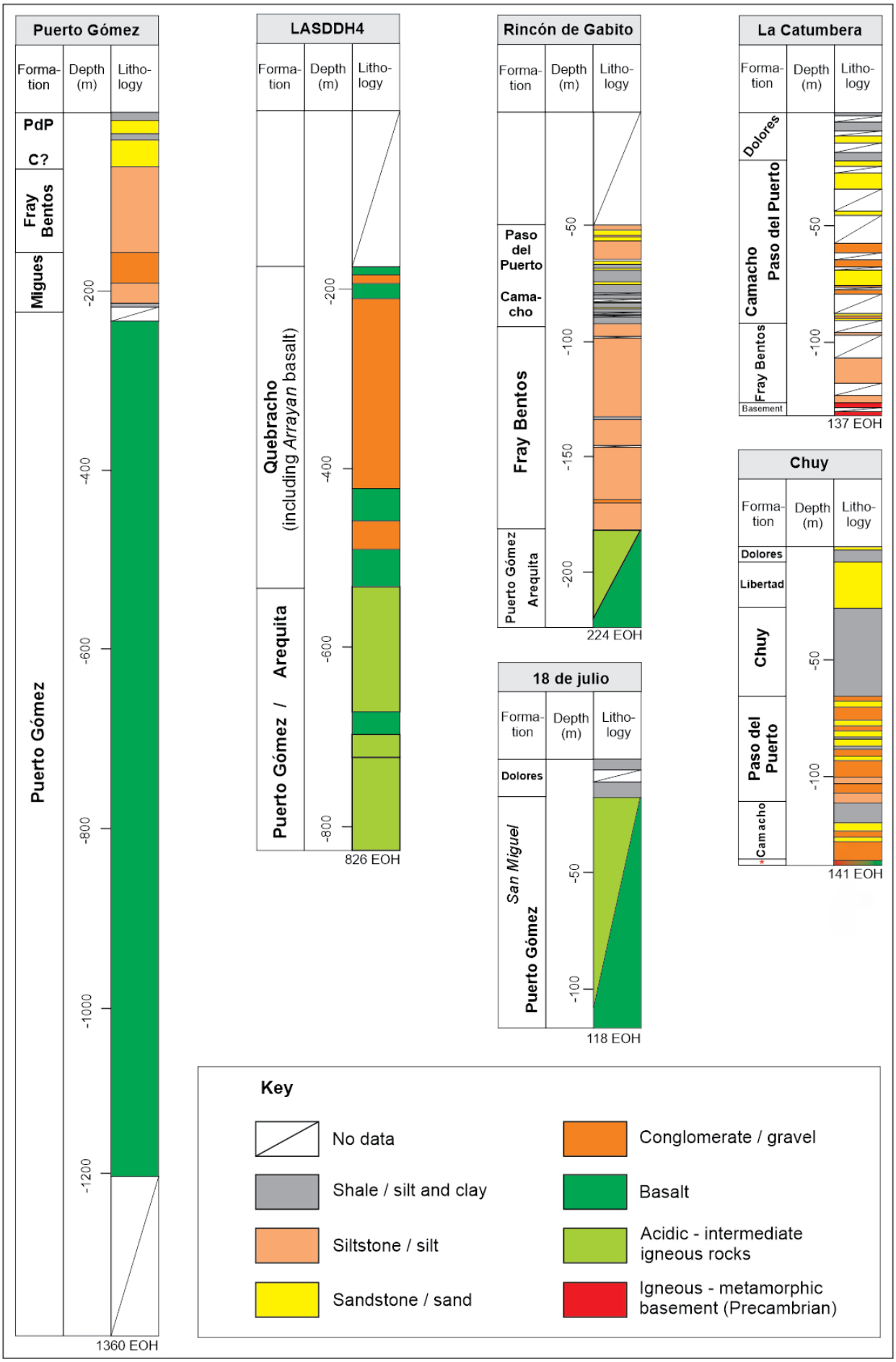

Source: modified from Cernuschi (2011), Cernuschi et al. (2015), Umpiérrez (2022), and Vivanco et al. (2020).

Figure 4. Lithostratigraphic profiles of selected wells of the LMB (see location in Figs. 3 and 9), including formal (bold) and unformal (italic) units. C, Camacho Formation; PdP, Paso del Puerto Formation; EOH, end-of-hole. (*) undefined crystalline rock.

between 1946 and 1978 by the National Agency of Mining and Geology (DINAMIGE), named Rincón de Gabito, La Catumbera, Chuy, 18 de Julio, and Puerto Gómez (Figs. 3 and 4). The Puerto Gómez well is the deepest well, with a total depth of 1,360 m, ending in the Mesozoic basaltic rocks. All of these "vintage" wells drilled the Mesozoic/Cenozoic sedimentary deposits with variable thicknesses between 220 m (Puerto Gómez well) and 18 m (18 de Julio well). Detailed lithostratigraphic descriptions of these wells are provided by Bossi (1966), Montaña and Bossi (1995), Umpiérrez (2022), and Vivanco et al. (2020). The 10 remaining deep wells were drilled between 2002 and 2008, with metallic mineral exploration purposes and variable depths between 450 and 1,040 m, ending in Mesozoic igneous rocks (basalts, gabbros, granodiorites, and rhyolites). Detailed lithostratigraphic descriptions can be found in Cernuschi (2011) and Cernuschi et al. (2015). All of them (with only one exception) were drilled in Mesozoic volcanic calderas, and no drillhole recovery of the sedimentary cover deposits was performed (see Cernuschi et al., 2015). The only well not drilled in the volcanic calderas is called LASDDH4 (Figs. 3 and 4), which was drilled just north of the Lascano Este Caldera and recovered almost 400 m of sedimentary rocks interbedded with igneous rocks.

In the Brazilian onshore portion of the basin, close to the border with Uruguay, four wells are located: 2-PJ-1-RS (Ponta do Joncal), 2-CA-1-RS (Curral Alto), 2-CI-1-RS (Cassino), and 2-PN-1-RS (Povo Novo) (see Fig. 1). Litho- and biostratigraphic descriptions were provided by Rosa et al. (2009) and Sanguinetti (1980).

A total of 49 groundwater wells (total depths less than 100 m) with available geological information were identified in the LMB (Fig. 3). Lithological descriptions have been provided by Medina and Pirelli (1995) and PRENADER (1993) (Fig. 3). These groundwater wells provide lithostratigraphic information on the sedimentary cover and, in some cases, their thickness, as many do not reach the underlying igneous rocks, ending in sedimentary rocks.

The geophysical data available in the study area, which can provide information about the sedimentary cover, include 13 long-range vertical electrical soundings (SEL) from Medina and Pirelli (1995) and 41 magnetotelluric (MT) station data from Morales et al. (2022) and Vivanco et al. (2020) (Fig. 3). These geophysical data provide information about the thickness of the sedimentary cover but do not allow discrimination between the different lithostratigraphic units.

All data were incorporated into a georeferenced project in the IHS Kingdom software to analyze the sedimentary cover and its isopach map.

4 SEDIMENTARY COVER THICKNESS

4.1 H/V Curves

The H/V curves obtained for the HVSR stations in this study were grouped into five types (Fig. 5).

- Type 1: The H/V curves are characterized by low H/V amplitudes (less than or equal to 2), except at low frequencies (near 1 Hz), where the ratio is higher. At all frequencies, no clear peak was identified, developing a curve that tended to be flat, probably because there was no strong impedance acoustic contrast between the basin layers. Station FC_11 (Fig. 5a) is an example of this type of curve. It is in an area of the Arequita Formation outcrop with acidic rhyolites and ignimbrites;
- Type 2: The H/V curves are characterized by a unique, clear peak of high H/V amplitudes (near 8) at frequencies near 3 Hz, corresponding to the fundamental resonance frequency of the surface layer. This peak is easily identifiable, as the H/V amplitudes for all the other frequencies are low (≤ a 2). An example of this type of H/V curve corresponds to station FC_12 (Fig. 5b), located on recent sediments, showing a high-impedance acoustic contrast between the sediment layers over the igneous rocks;
- Type 3: The H/V curves have similar characteristics to the previous one, consisting of a unique clear peak at frequencies near 3 Hz, but in this case, with an intermediate H/V amplitude (near 5), which also represents a significant contrast in acoustic impedance between the layers in the basin. An example of this type of H/V curve is station FC_13 (Fig. 5c). The acoustic impedance contrast was greater at station FC_12 than at station FC_13, which is consistent with the geology. While the FC_12 station shows the contrast between "softer" recent sediments and the igneous rocks, the FC_13 shows an impedance acoustic contrast between "harder" Late Pleistocene sediments (Dolores Formation) than modern sediments and the igneous rocks, thus developing a smaller peak;
- Type 4: The H/V curves are characterized by a mostly flat curve without a clear peak. It is like the first type described, but in this case, with low H/V amplitudes (≤ a 1) for the entire frequency range without evidencing a marked acoustic impedance contrast between the basin layers. An example of this type of curve corresponds to the FC_34 station (Fig. 5d), located on Pliocene-Pleistocene sediments (Paso del Puerto Formation). However, according to groundwater well data from the area, igneous rocks are present at very shallow depths. The absence of acoustic impedance contrast in this area may be associated with the very thin sediment layer (only 4 m of sediment in the groundwater well #2172 from Medina & Pirelli, 1995);
- Type 5: The H/V curves are characterized by the presence of two peaks, a wide peak in frequencies near 0.1 Hz and a clear peak located in frequencies near 3 Hz, both with high H/V amplitudes (near 8) and easily identifiable given that the H/V amplitudes are low for all the other frequencies (≤ a 2). An example of this H/V curve corresponds to station FC_35 (Fig. 5e). The two peaks corresponded to at least three layers with different mechanical behaviors, two existing interfaces with a high acoustic impedance contrast, and deeper contact corresponding to lower frequencies. Long-range vertical electrical sounding (SEL #10 from Medina & Pirelli, 1995) revealed the presence of several layers with different

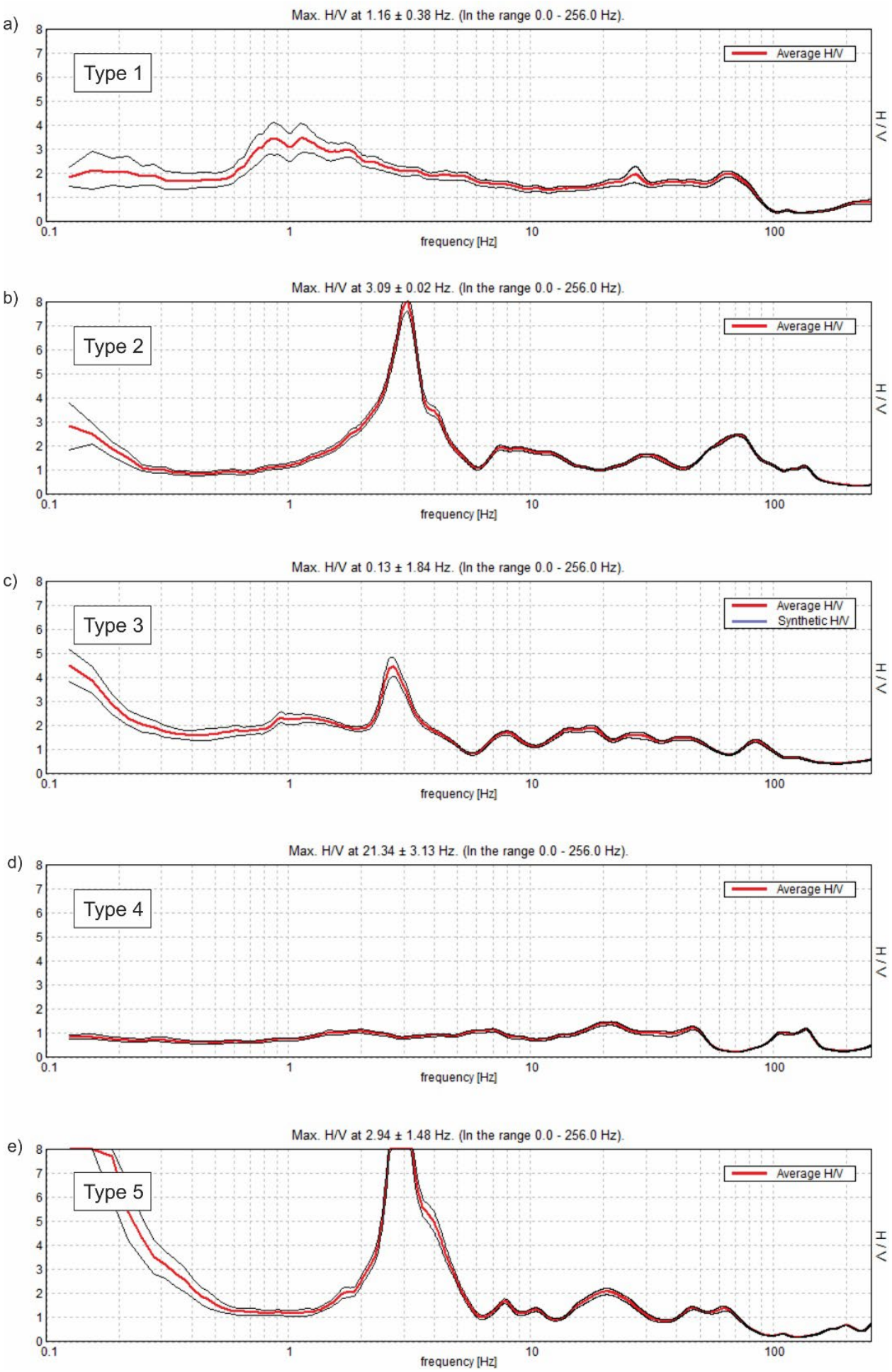

Figure 5. Type H/V curves for HVSR stations: (a) FC_11; (b) FC_12; (c) FC_13; (d) FC_34; (e) FC_35.

resistivities. This could explain the development of more than one H–V curve peak. Station FC_35 was located in the Dolores Formation sediments, consistent with at least one peak corresponding to the sediment/hard rock interface.

4.2 HVSR 2D transects (frequency and depth)

From the 58 HVSR-acquired stations, five 2D transects (A–E; Fig. 3) were selected and processed in terms of frequency (Fig. 6) and depth (Fig. 7). Transects A and C SW-NE are 53 and 30 km long, respectively. Transects B, D, and E NW-SE transects had 64, 62, and 30 km lengths, respectively. Figures 6 and 7 also indicate the locations of the available geological and geophysical data along each or very close to the transects, with which the interpretation of the base of the sedimentary cover was contrasted.

The boundary between the soil and sedimentary cover (sediments/sedimentary rocks) of the basin was identified in the HVSR transects processed in frequency (blue horizon in Fig. 6). This boundary is located at frequencies near 10^2 Hz and is represented by a reflector with low to intermediate amplitudes (2-4). The soil layer was homogeneous and had an amplitude near zero. This layer was also identified in all groundwater wells of the study area, as described by Medina and Pirelli (1995) and PRENADER (1993). It has a maximum thickness of 1 m and is composed mainly of silt and clay grains with a high organic matter content.

The boundary between "soft" (sediments/sedimentary rocks) and "hard" rocks (igneous rocks) corresponds to the pink horizon in Fig. 6. It is also recognized in all HVSR frequency transects and is represented by a subhorizontal reflector with intermediate to high amplitudes (4-6). This horizon is absent where igneous rock outcrops, as it occurs in the central segment of transects A, B, and C. This horizon is recognized along Transect E, located entirely on Cenozoic sedimentary cover. The presence of isolated reflectors inside the sedimentary cover, with amplitude values between 2 and 4, could represent the interfaces between different sedimentary layers, which have been identified in the sedimentary cover of the "vintage" wells described by Umpiérrez (2022) and Vivanco et al. (2020) and groundwater wells described by Medina and Pirelli (1995) and PRENADER (1993).

The soil-sedimentary cover (sediments/sedimentary rocks) boundary was not distinguished in the HVSR transects processed at depth (Fig. 7) because of the very low thickness of the soil layer. At the same time, the boundary between "soft" (sediments/sedimentary rocks) and "hard" rocks (igneous rocks), corresponding to the pink horizon in Fig. 7, is interpreted with typically 0.4–0.8 H/V log values and variable depths between 20 m and more than 100 m. It is absent where igneous rocks outcrop.

The boundary between "soft" (sediments/sedimentary rocks) and "hard" rocks (igneous of the infill basin or igneous/metamorphic basement rocks) was also recognized in all the stratigraphic wells (Sanguinetti, 1980; Umpiérrez, 2022; Vivanco et al., 2020), all the MT data (Morales et al., 2022; Vivanco et al., 2020), all the SEL data (Medina & Pirelli, 1995), and some groundwater wells (Medina & Pirelli, 1995; PRENADER, 1993).

Anomalies (white ovals in dotted lines in Figs. 6 and 7) were observed in the frequency and depth of HVSR transects in the layer corresponding to igneous rocks. These anomalies appear at frequencies < 100 Hz and depths between 200 m and 400 m, with high amplitude values around 7 and high log H/V values (between 0.6 and 1), respectively. They could have different explanations, such as 2D or 3D structural behaviors in zones with high slopes in the subsurface due to the proximity of complex structures such as volcanic calderas and/or regional lineaments (Agostini et al., 2015; Lane et al., 2008), both of which are features present in the LMB.

4.3 Isopach map

The top of the sedimentary cover in the LMB is represented by Cenozoic units deposited from the Pliocene to modern fluvial and alluvial deposits. It is characterized by a flat topography with elevations predominantly between 5 and 10 m above sea level (msl), with the Merín Lagoon being the current base level of the basin. In the western region of the basin, the top of the sedimentary cover is situated at higher elevations, ranging from approximately 40 to 80 msl (Paso del Puerto and Libertad Formations outcrops).

The base of the sedimentary infill is located at its greatest depth in the central region of the basin, between the CML and AICL, and is generally between 190 and 290 mbsl. Its maximum depth (490 mbsl) is in the basin depocenter to the east, near the Merín Lagoon. In the remaining sectors of the LMB, the base of the sedimentary cover was located near 30 mbsl. Exceptionally, the base of the sedimentary cover reaches higher altitudes, such as to the west, next to Mesozoic volcanic rock outcrops or basin borders.

Figure 8 presents an isopach map of the sedimentary infill of the LMB, whose thickness increases eastward along the structural boundaries of the basin. The greatest sedimentary thickness was identified in the eastern sector of the basin between the CML and AICL, north of the San Luis River and the Pelotas Stream lineaments. In this region, the sedimentary cover thickness varies mostly between 150 and 300 m, reaching a maximum value of 500 m. Between the CML and the Olimar-Tacuarí lineament, the sedimentary cover thickness has a mean value of 150 m. Toward the borders of the LMB, the sedimentary thickness is lesser (between 50 and 100 m), with the smallest thicknesses (less than 50 m) in the LMB's western area, next to basement outcrops and on the edges of volcanic hills.

The greatest sedimentary infill thickness is located north of the Lascano West and Lascano East volcanic complexes and over the San Luis volcanic caldera, as characterized by Cernuschi et al. (2015). Unlike the Lascano East and Lascano West volcanic calderas (Cernuschi et al., 2015), the San Luis volcanic caldera has no outcropping areas, has been identified using geophysical data (gravimetry and magnetometry), and constitutes a mostly floodable area.

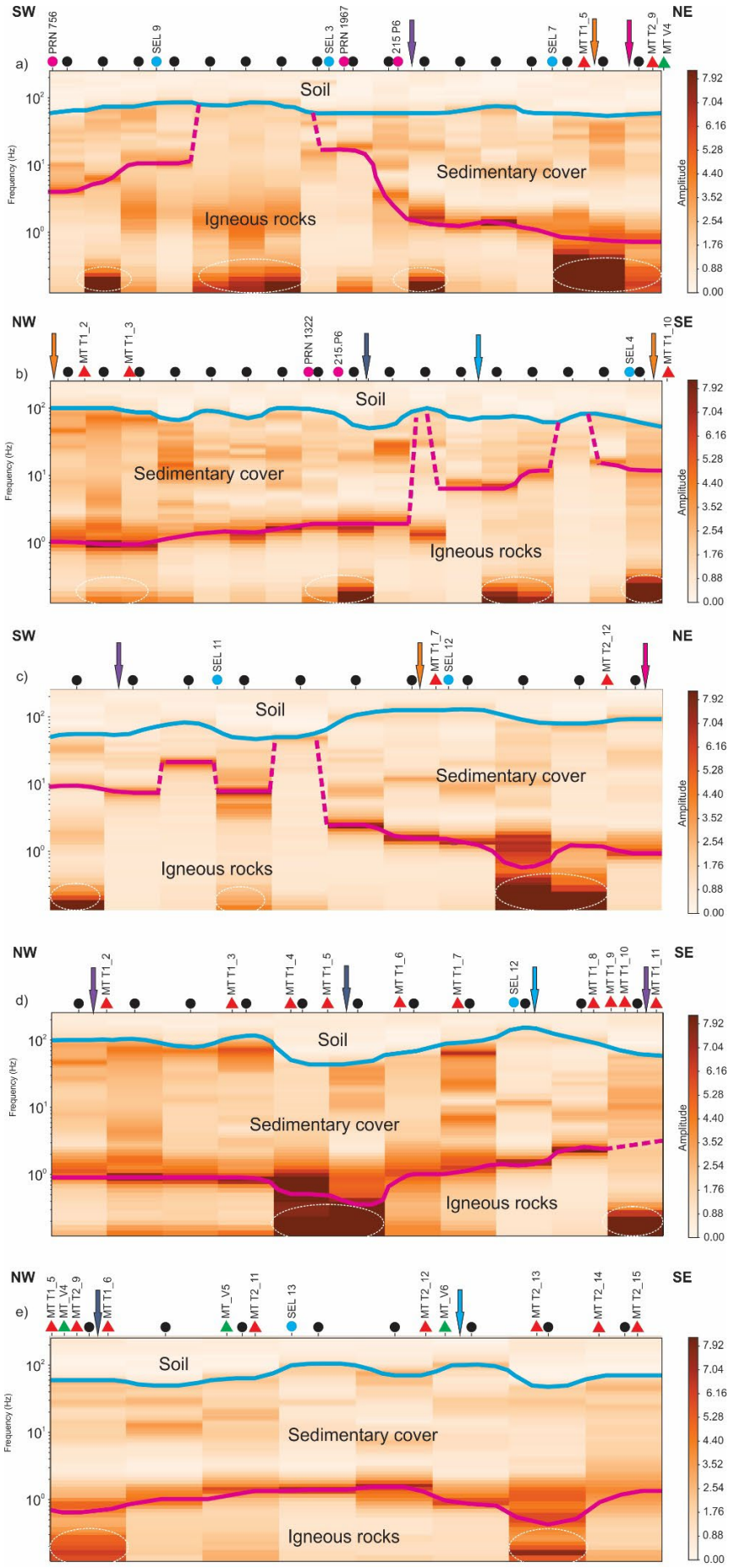

Figure 6. HVSR transects in frequency (Hz): (a) transect A; (b) transect B; (c) transect C; (d) transect D; (e) transect E. Blue arrow, intersection with transect A location; purple arrow, intersection with transect B location; sky blue arrow, intersection with transect C location; orange arrow, intersection with transect D location; pink arrow, intersection with transect E location. See the location and symbology of geological and geophysical data in Fig. 3. White ovals in the dotted line indicate anomalies in the layer of igneous rocks.

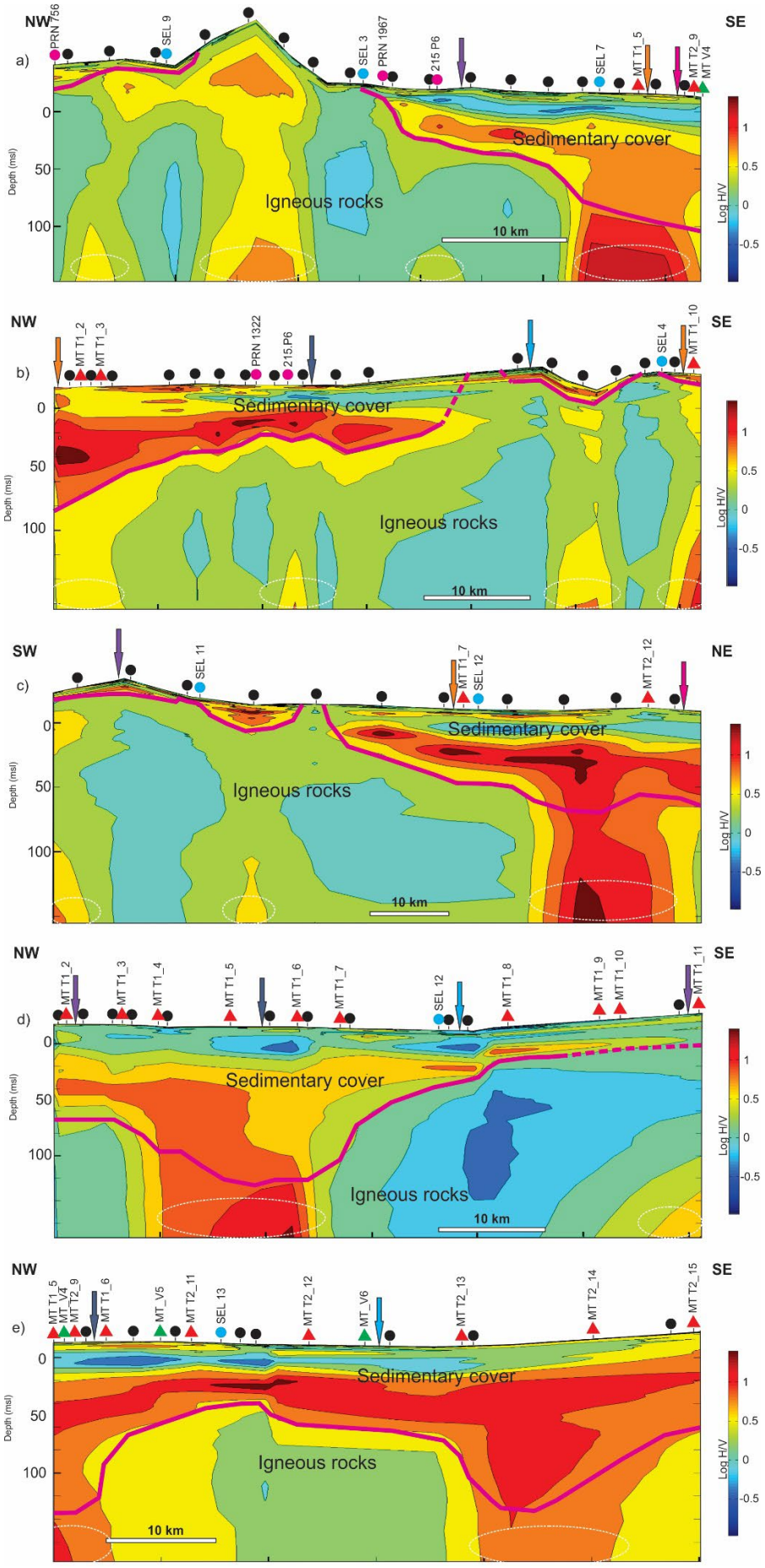

Blue arrow: intersection with transect A location; purple arrow: intersection with transect B location; sky blue arrow: intersection with transect C location; orange arrow: intersection with transect D location; pink arrow: intersection with transect E location.

Figure 7. HVSR transects in depth (m): (a) transect A; (b) transect B; (c) transect C; (d) transect D; (e) transect E. See the location and symbology of geological and geophysical data in Fig. 3. White ovals in the dotted line indicate anomalies in the layer of igneous rocks.

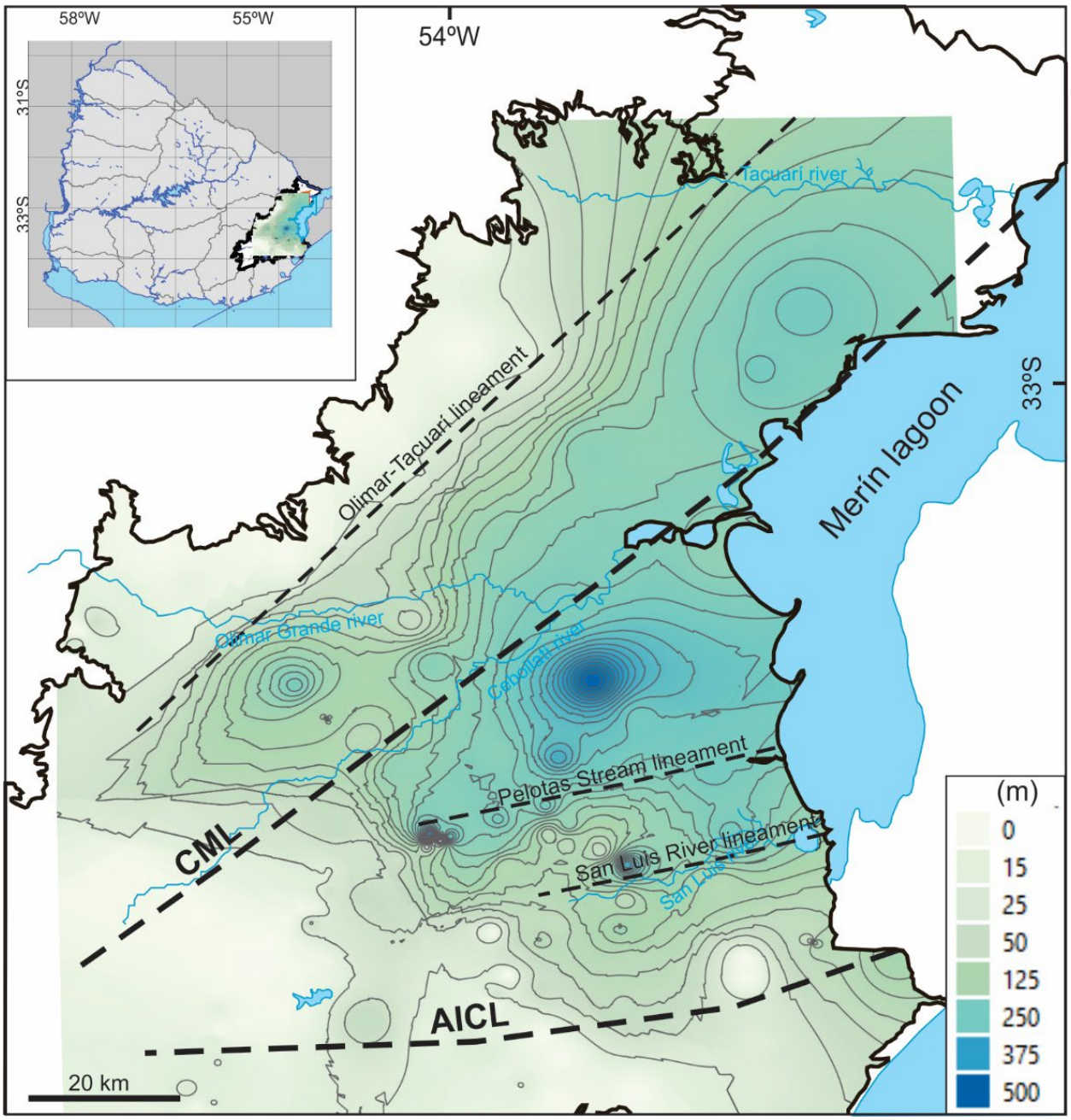

AICL: Aiguá-India Muerta-Chuy Lineament; CML: Cebollatí-Merin Lineament.
Figure 8. Isopach map (m) of the Laguna Merín Basin sedimentary infill. The main lineaments are indicated.

5 GEOLOGICAL EVOLUTION OF THE SEDIMENTARY INFILL

The sedimentary infill of the LMB is represented by Mesozoic/Cenozoic sedimentary rocks and sediments deposited during the rift and drift tectonic phases of evolution (Figs. 2 and 9).

The rift sedimentary facies of the LMB are recognized in very few outcrops (represented by alluvial deposits) located in the western sector of the basin, close to the basement highs of the basin´s border. They were only identified in the Puerto Gómez well (represented by fluvial deposits), covering the basalts of the Puerto Gomez Formation. Cernuschi et al. (2015) identified in the LASDDH4 well conglomerates with a thickness of slightly less than 400 m (defined by these authors as the Quebracho Formation). These conglomerates are interbedded with basalts of the rift phase; therefore, a Barremian-Aptian age is proposed for them. Also, Morales et al. (2022) interpreted sedimentary or volcano-sedimentary deposits as conductive layers interbedded with more resistive layers (basalts) that could correspond to sedimentary rift phase deposits.

The end of the rift phase in the Pelotas Basin occurred around 110 Ma, evolving to a passive margin basin type up to the present day, exhibiting a gradual decrease in the subsidence rate for the offshore region from the Early Cretaceous and reaching a minimum during the Cretaceous-Paleogene (Contreras et al., 2010; Fontana, 1996). From the Early Cretaceous to the Oligocene, there were no sedimentary deposits in the LMB, probably due to the absence of accommodation space. Although very little thermochronological

data are available for Uruguay, they show a complex history with a slow and continuous cooling episode in the eastern region (DFB) starting in the Cretaceous (Machado et al., 2021; Gomes & Almeida, 2019).

During the Eocene (~ 40 Ma), a denudation episode is characterized for southeast Uruguay and Brazil (Gomes & Almeida, 2019), which may be correlated to the formation of the Rio Grande Cone in the Brazilian offshore Pelotas (Fontana, 1996). During this period, there was a substantial increase in detrital input to the continental margin (Barboza et al. 2011; Morales et al., 2017), with the consequent progradation of several deltaic systems over time (Conti et al., 2017; Morales et al., 2017).

The oldest Cenozoic deposits in the LMB correspond to the Oligocene Fray Bentos Formation (Figs. 2 and 10), which is composed of continental fine and very fine-grained clastic

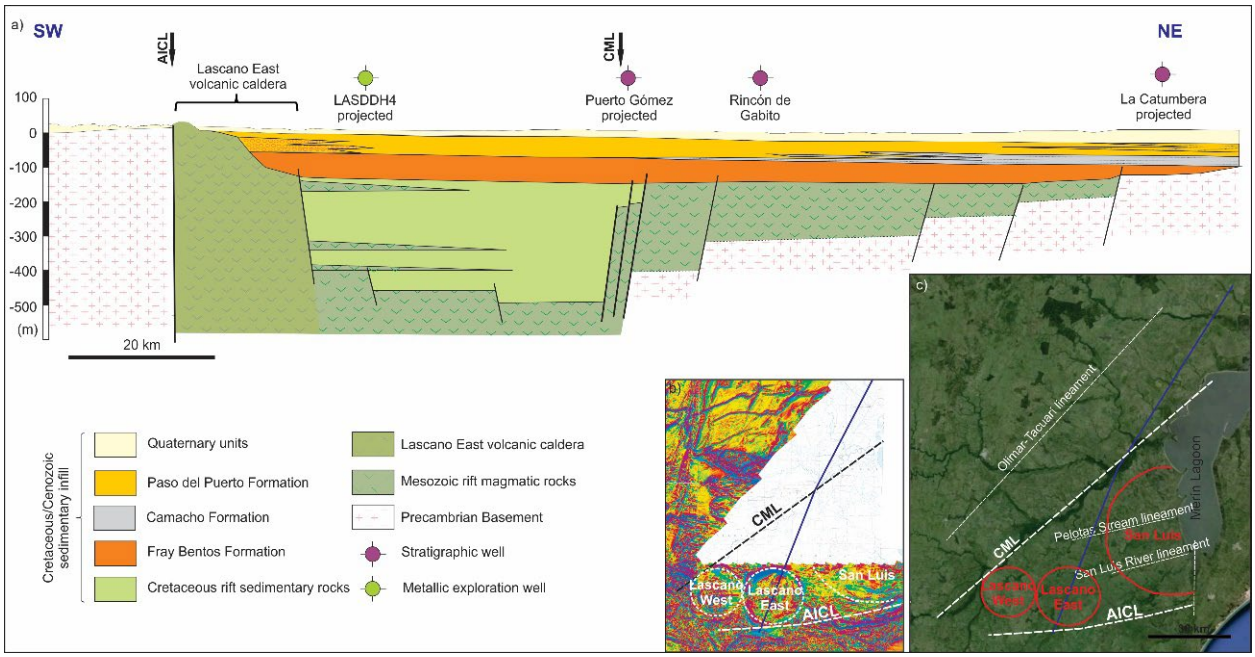

AICL: Aiguá-India Muerta-Chuy Lineament; CML: Cebollatí-Merin Lineament.

Figure 9. (a) Geological cross-section of the Laguna Merín Basin until 500 m depth (blue line in b and c) (see lithostratigraphic profiles in Fig. 4); (b) aero-magnetometry (DINAMIGE, 2018), showing the Lascano West, Lascano East, and San Luis volcanic calderas locations; (c) satellite image from Google Earth, showing the Lascano West, Lascano East, and San Luis volcanic calderas locations and main structural lineaments.

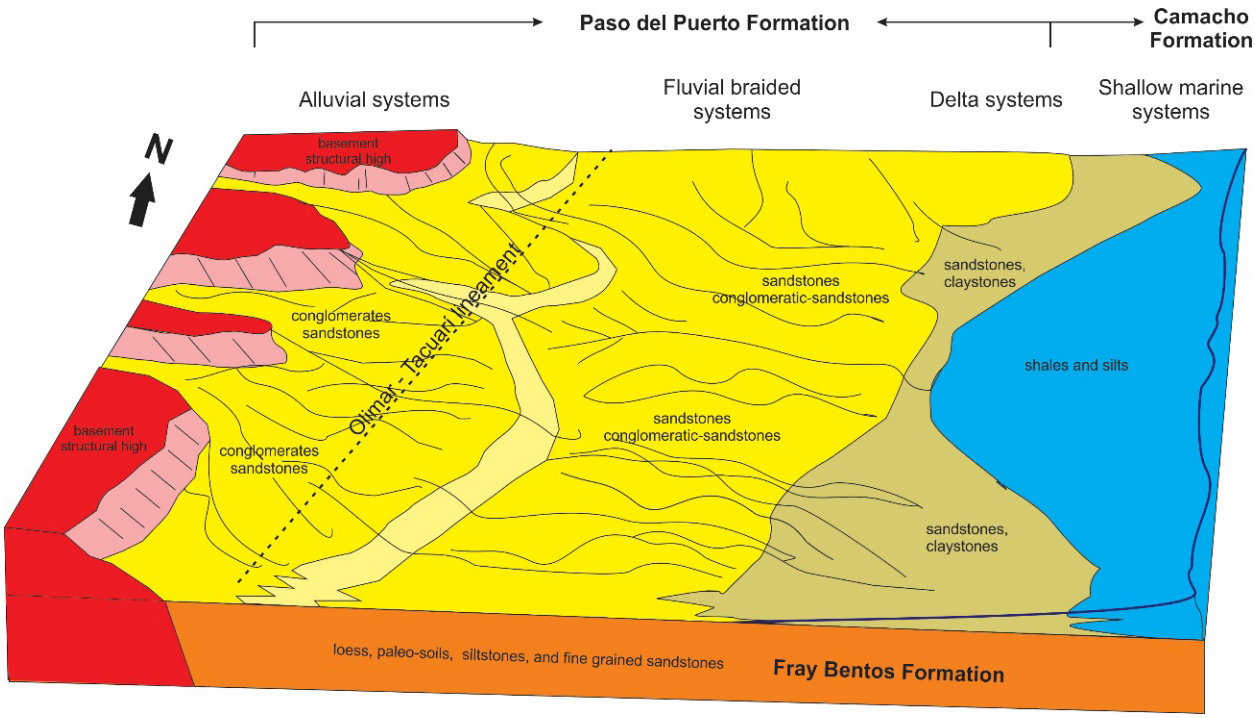

Figure 10. Schematic block diagram showing the paleogeography of the LMB during the Late Miocene-Pliocene and the underlying uniform Oligocene interval.

rocks and loess with paleo-soils and caliche beds. This unit is absent in the Chuy and 18 de Julio wells, located at the southeastern border of the basin, and in the wells located in the onshore Brazilian portion of the basin close to Uruguay. This sedimentation developed over most of the LMB (Figs. 9 and 10) with a mean thickness of 90 m, likewise throughout Uruguay. The absence of this unit toward the southeast could be due to the presence of an N-S structure (Fig. 9), coinciding with the N-S segment of the Merín Lagoon. The difference in the thickness of the sedimentary cover in the 18 de Julio (18 m) and Chuy (140 m) wells (Figs. 3 and 4), separated by only 8 km, also suggests the presence of this N-S structure.

During the Miocene, in the context of the greater stability of southern Uruguay (Gomes & Almeida, 2019; Machado et al., 2021), a marine transgression from the east was recorded and documented by the presence of fossiliferous (including gastropods, clams, bivalves, foraminifera, and ostracods) fine-grained siliciclastic deposits (Sprechmann et al., 2000). Sanguinetti (1980) described Miocene deposits directly over the basement in the 2-PJ-1-RS, 2-CI-1-RS, and 2-PN-1-RS wells located in Rio Grande do Sul (Brazil) with a thickness between 156 and 522 m. The 2-CA-1-RS well drilled 320 m of Miocene sediments, but it did not reach the basement. In the LMB, Miocene sediments with a mean thickness of 60, increasing to the east, were drilled in the La Catumbera, Rincón de Gabito, Puerto Gómez, and Chuy wells, and groundwater wells located in the eastern sectors of the basin. The paleoshoreline would be close to the longitude of the Puerto Gómez well because the wells located in the WNW have no drilled marine Miocene deposits.

The thick layers identified in the geophysical data (mainly MT from Morales et al., 2022; and Vivanco et al., 2020), with high conductivity and thickness greater than 100 m, located between the CML and Olimar-Tacuarí lineament, could be interpreted as coarse-grained proximal alluvial and fluvial deposits (referred to as Paso del Puerto Formation in outcrops or shallow depths) interdigitated with the marine strata of the Camacho Formation (Figs. 9 and 10). According to their location, continuity, and stratigraphic position, they can be correlated with the alluvial fan systems developed along the basement structural highs in the southeast of Rio Grande do Sul, as described by Tomazelli and Villwock (2000) for the Brazilian Pelotas onshore. The Paso del Puerto Formation has a maximum drilled thickness of 40 m, recognized in several groundwater wells by Medina and Pirelli (1995) and PRENADER (1993), with a mean thickness of 20 m. Thus, the thickness of these layers identified from the geophysical data is twice or three times the drilled thickness and probably the result of the structural control of the Olimar-Tacuarí lineament associated with the basement heights at the basin border.

During the Quaternary, sedimentation in the LMB was controlled by the current geographical framework, very slow subsidence, and sea level oscillations, with the alternation of continental systems represented by fluvial deposits and coastal to marine systems. The Quaternary Libertad (Lower Pleistocene) and Dolores (Upper Pleistocene) formations represent the most important continental deposits, with a maximum thickness of 40 m. In contrast, the Chuy (Upper Pleistocene) and Villa Soriano (Holocene) formations represent transitional to marine deposits, with a maximum thickness of 20 m. Finally, modern sediments are associated with the most important alluvial and fluvial system-built terrace levels and plains.

6 CONCLUSIONS

The results obtained in this study contribute to improving regional geological knowledge of the Uruguayan onshore region of the Pelotas Basin. The characteristics, areal extension, and thickness of the sedimentary infill of the Uruguayan onshore portion were established to better understand the structural controls and spatial distribution of the magmatic-sedimentary infill of the basin.

The scarcity of outcrops and well data in the LMB, together with the strong impedance contrast of the rock sequences in its infill, make the use of the HVSR geophysical method a valuable tool for defining the distribution of different groups of rocks (e.g., igneous and sedimentary) and their thickness.

The Cretaceous rift sedimentary deposits (alluvial and fluvial) are restricted between the rifting structural borders (CML and AICL). Besides, the drift deposits present a regional areal extension that exceeds the structural rifting borders of the basin, although the Olimar-Tacuarí lineament has exerted an important control over the Cenozoic sedimentation. A depocenter with the greatest thickness of approximately 500 m was identified between the CML and AICL, close to Merín Lagoon and to the north of the Lascano East and Lascano West volcanic calderas.

Defining the spatial distribution of Cretaceous and Cenozoic sedimentation in the LMB could contribute to establishing future groundwater research guidelines to support the various economic activities carried out in the basin (mainly rice cultivation).

The Brazilian and Uruguayan onshore regions of the Pelotas Basin exhibited significant differences. Cretaceous magmatic and sedimentary units related to the rift and Oligocene drift phases are present in the Uruguayan onshore portion of the basin and are absent in the Brazilian portion. The thickness of the Cenozoic drift deposits (from the Miocene to modern deposits) in the Brazilian region is at least twice that in the Uruguayan onshore region.

ACKNOWLEDGMENTS

The authors would like to thank IHS for granting a Kingdom software license to the Instituto de Ciencias Geológicas of Universidad de la República, to the Dirección Nacional de Minería y Geología (DINAMIGE, MIEM) for allowing access to the "vintage" wells, and to the reviewers for their valuable comments and suggestions.

ARTICLE INFORMATION
Manuscript ID: 20240017. Received on: 5 APR 2024. Approved on: 30 SEP 2024.

How to cite: (2024). Unveiling the sedimentary infill of the Uruguayan onshore portion of the Pelotas Basin (southeast of Uruguay). *Brazilian Journal of Geology*, *54*(2):e20240017. https://doi.org/10.1590/2317-4889202420240017

E.M.: Conceptualization, Methodology, Investigation, Writing, Visualization. G.V.: Methodology, Investigation, Writing, Visualization. R.U.: Methodology, Investigation, Writing, Visualization. J.M.: Methodology, Investigation, Writing. F.P.: Methodology, Investigation. B.C: Investigation, Writing.

This study contributes to the framework of the Agencia Nacional de Investigación e Innovación (ANII) Project 'Evaluación preliminar del potencial hidrocarburífero de la Cuenca Laguna Merín' (FSE 2017-1447979).

Conflict of interest: On behalf of all authors, the corresponding author states that there is no conflict of interest.

REFERENCES

Achkar, M., Domíngez, A., & Pesce, F. (2012). *Ecorregiones del Uruguay*. Technical report (unpublished). MGAP/PPR – CIEDUR/Facultad de Ciencias/Vida Silvestre Uruguay/Sociedad Zoológica del Uruguay.

Agostini, L., Boaga, J., Galgaro, A., & Ninfo, A. (2015). HVSR technique in near-surface thermal- basin characterization: the example of the Caldiero district (North-East Italy). *Environmental Earth Sciences*, *74*(2), 1199-1210. http://dx.doi.org/10.1007/s12665-015-4109-0

Barboza, E. G., Rosa, M. L. C. C., Hesp, P. A., Dillenburg, S. R., Tomazelli, L. J., & Ayup-Zouain, R. N. (2011). Evolution of the Holocene Coastal Barrier of Pelotas Basin (Southern Brazil): a new approach with GPR data. *Journal of Coastal Research*, 646-650. http://www.jstor.org/stable/26482251

Bard, P.-Y. (1998). Microtremor measurements: A tool for site effect estimation? In: 2nd *International Symposium on the Effects of Surface Geology on Seismic Motion*. Yokohama, *3*, 1251-1279.

Bossi, J. (1966). *Geología del Uruguay*. Departamento de Publicaciones, Universidad de la República.

Bossi, J., Campal, N., Hartman, L. A., Schipilov, A., & Piñeyro, D. (2001). Thirty-five years or geochronology in Uruguay. In: 3er *Congreso Uruguayo de Geología*, Montevideo, Uruguay.

Bossi, J., & Gaucher, C. (2004). The Cuchilla Dionisio Terrane, Uruguayan allochthonous block accreted in the Cambrian to SW Gondwana. *Gondwana Research*, *7*(3), 661-674. https://doi.org/10.1016/S1342-937X(05)71054-6

Bossi, J., & Navarro, R. (1991). *Geología del Uruguay*. Departamento de Publicaciones, Universidad de la República.

Bueno, V. G. (2021). Bacia de Pelotas em retrospectiva. In: Jelinek, A. R., & Sommer, C. A. (eds.), *Contribuições à Geologia do Rio Grande do Sul e de Santa Catarina* (pp. 397-410). Compasso Lugar Cultura.

Cernuschi, F. (2011). *Geology of the Cretaceous Lascano-East intrusive complex: magmatic evolution and mineralization potential of the Merin Basin, Uruguay* (Master Thesis). Oregon State University. Retrieved from https://ir.library.oregonstate.edu/concern/graduate_thesis_or_dissertations/cr56n327j

Cernuschi, F., Dilles, J. H., Kent, A. J. R., Schroer, G., Raab, A. K., Conti, B., & Muzio, R. (2015). Geology, geochemistry and geochronology of the Cretaceous Lascano East intrusive complex and magmatic evolution of the Laguna Merín basin, Uruguay. *Gondwana Research*, *28*(2), 837-857. https://doi.org/10.1016/j.gr.2014.07.007

Chang, H. K., Kowsmann, R. O., Figueiredo, A. M. F., & Bender, A. A. (1992). Tectonics and stratigraphy of the East Brazil Rift system: an overview. *Tectonophysics*, *213*(1-2), 97-138. https://doi.org/10.1016/0040-1951(92)90253-3

Chauvet, F., Sapin, F., Geoffroy, L., Ringenbach, J. C., & Ferry, J. N. (2021). Conjugate volcanic passive margins in the austral segment of the South Atlantic–Architecture and development. *Earth-Science Reviews*, *212*, 103461. https://doi.org/10.1016/j.earscirev.2020.103461

Conti, B., Perinotto, J. A., Veroslavsky, G., Castillo, M.G., de Santa Ana, H., Soto, M., & Morales, E. (2017). Speculative petroleum systems of the southern Pelotas Basin, offshore Uruguay. *Marine and Petroleum Geology*, *83*, 1-25. https://doi.org/10.1016/j.marpetgeo.2017.02.022

Contreras, J., Zühlke, R., Bowman, S., & Bechstädt, T. (2010). Seismic stratigraphy and subsidence analysis of the southern Brazilian margin (Campos, Santos and Pelotas basins). *Marine and Petroleum Geology*, *27*(9), 1952-1980. https://doi.org/10.1016/j.marpetgeo.2010.06.007

de Santa Ana, H., Veroslavsky, G., Fulfaro, V. J., & Rossello, E. (2006). Evolución tectónica y sedimentaria del Carbonífero – Pérmico de la Cuenca Norte. In: Veroslavsky, G., Ubilla, M., & Martínez, S. (eds.), *Cuencas Sedimentarias de Uruguay: geología, paleontología y recursos naturales – Paleozoico* (pp. 209-256). DIRAC, Facultad de Ciencias.

Dirección Nacional de Minería y Geología (DINAMIGE). (2018). *Aeromagentometría-Vuelo Nacional 2017-2018*. DINAMIGE. Retrieved from https://visualizadorgeominero.dinamige.gub.uy/Dinamige_MVC2/

Ellis, T., & Turner, R. (2006). *Progress report on the evaluation of the air-FTG gravity gradiometer and aeromagnetic surveys on the Lascano project, Uruguay*. Technical report (unpublished). Orosur Mining INC.

Fontana, R. L. (1996). *Geotectônica e sismoestratigrafia da Bacia de Pelotas e Plataforma de Florianopolis* (PhD thesis). Universidade Federal do Rio Grande do Sul.

Gomes, C. H., & Almeida, D. (2019). New insights into the Gondwana breakup at the Southern South America by apatite fission-track analyses. *Advances in Geoscience*, *47*, 1-15. https://doi.org/10.5194/adgeo-47-1-2019.

Gómez-Rifas, C. (1995). *A Zona de Cisalhamento sinistral de Sierra Ballena no Uruguai* (PhD thesis). Instituto de Geociências da Universidade de São Paulo.

Goscombe, B., Hand, M., Gray, D., & Mawby, J. (2003). The metamorphic arquitecture of a tranpressional Orogen: The Kaoko Belt, Namibia. *Journal of Petrology*, *44*(4), 679-711. https://doi.org/10.1093/petrology/44.4.679

Goso, H. (1972). *El Cuaternario Uruguayo*. Programa de Estudio y Levantamiento de Suelos. Ministerio de Agricultura y Pesca.

Goso, H. (1985). *El Cenozoico en el Uruguay*. Technical report (unpublished). Instituto Geológico del Uruguay.

Lane, J., White, E., Steele, G., & Cannia, J. (2008). Estimation of bedrock depth using the horizontal-to-vertical (H/V) ambient-noise seismic method. In: *Symposium on the Application of Geophysics to Engineering and Environmental Problems*, April 6-10, 2008, Philadelphia. Proceedings: Denver, Colorado, Environmental and Engineering Geophysical Society.

Machado, J. P. S, Stephenson, R., Jelinek, A., & Abdallah, R. (2021). Sismoestratigrafía e evolução da Bacia de Pelotas. In: Jelinek, A. R., & Sommer, C. A. (eds.), *Contribuições à Geologia do Rio Grande do Sul e de Santa Catarina*. Compasso Lugar Cultura.

Martínez, S., & Ubilla, M. (2004). El Cuaternario de Uruguay. In: Veroslavsky, G., Ubilla, M., & Martínez, S. (eds.), *Cuencas Sedimentarias de Uruguay: geología, paleontología y recursos naturales – Cenozoico* (pp. 195-228). DIRAC, Facultad de Ciencias.

Martins Neto, M. A., Falkenhein, F., Cupertino, J. A., Marques, E. J. J., Bueno, G. V., Porsche, E., Barbosa, M. S. C., Gomes, N. S., Ev, L. F., & Leite, M. G. P. (2006). Breakup propagation in Pelotas basin, southern Brazil. In: *Congresso Brasileiro de Geologia*, 43, 2006, Aracaju. Anais. SBG, *2*, AO16.

Masquelin, H. (2006). El Escudo uruguayo. In: Veroslavsky, G., Ubilla, M., & Martínez, S. (eds.), *Cuencas Sedimentarias de Uruguay: geología, paleontología y recursos naturales – Paleozoico* (pp. 37-106). DIRAC, Facultad de Ciencias.

Medina, E., & Pirelli, H. (1995). *Anomalía gravimétrica de la Cuenca Laguna Merín*. Misión geofísica alemana. Internal report (unpublished). División geofísica, Dirección Nacional de Minería y Geología.

Montaña, J., & Bossi, J. (1995). *Geomorfología de los humedales de la Cuenca Laguna Merín en el departamento de Rocha*. Facultad de Agronomía, Universidad de la República.

Morales, E., Chang, H. K., Soto, M., Santos Corrêa, F., Veroslavsky, G., de Santa Ana, H., Conti, B., & Daners, G. (2017). Tectonic and stratigraphic evolution of the Punta del Este and Pelotas Basins (offshore Uruguay). *Petroleum Geoscience*, *23*(4), 415-426. https://doi.org/10.1144/petgeo2016-059

Morales, E., Plenc, F., Marmisolle, J., Rossello, E., Oleaga, A., & Umpiérrez, R. (2022). Tectono-stratigraphic evolution of the Jurassic-Cretaceous Laguna Merín Basin (Uruguay): new insights from magnetotellurica transects. *Tectonophysics*, *823*, 229211. https://doi.org/10.1016/j.tecto.2022.229211

Muzio, R. (2000). *Evolução petrológica e geocronológica do Maciço Alcalino Valle Chico, Uruguai* (PhD thesis). Instituto de Geociências e Ciências Exatas, Universidade Estadual Paulista "Júlio de Mesquita Filho".

Muzio, R., Peel, E., & Morales, E. (2009). Mesozoic magmatism in East Uruguay: petrological constraints related to the Sierra de San Miguel region. *Earth Sciences Research Journal*, *13*(1), 16-29.

Nuñez Demarco, P., Masquelin, H., Prezzi, C., Aïfa, T., Muzio, R., Loureiro, J., Peel, E., Campal, N., & Sánchez Bettucci, L. (2020). Aeromagnetic patterns in Southern Uruguay: Precambrian-Mesozoic dyke swarms and Mesozoic rifting structural and tectonic evolution. *Tectonophysics*, *789*, 228373. https://doi.org/10.1016/j.tecto.2020.228373

Owers, M. C., Meyers, J. B., Siggs, B., & Shackleton, M. (2016). Passive seismic survey for depth to base of paleochannel mapping at Lake Wells, Western Australia. In: 25th *Geophysical Meeting*, ASEG-PESA-AIG.

Oyhantçabal, P., Siegesmund, S., & Wemmer, K. (2011). The Rio de la Plata Craton: a review of units, boundaries, ages and isotopic signature. *International Journal of Earth Science*, *100*(2-3), 201-220. https://doi.org/10.1007/s00531-010-0580-8

Panario, D. (1988). *Geomorfología del Uruguay*. Facultad de Humanidades y Ciencias, Universidad de la República.

Perea, D., & Martínez, S. (2004). Estratigrafía del Mioceno–Pleistoceno en el litoral sur-oeste de Uruguay. In: Veroslavsky, G., Ubilla, M., & Martínez, S. (eds.), *Cuencas Sedimentarias del Uruguay. Geología, paleontología y recursos minerales. Cenozoico* (pp. 105-124). DIRAC, Facultad de Ciencias.

Preciozzi, F., Spoturno, J., Heinzen, W., & Rossi, P. (1985). *Carta geológica del Uruguay a escala 1:500.000*. Dirección Nacional de Minería y Geología.

Programa de Manejo de Recursos Naturales y Desarrollo del Riego (PRENADER) (1993). *Internal report* (unpublished). Ministerio de Ganadería, Agricultura y Pesca.

Reitmayr, G. (2001). Una espectacular peculiaridad uruguaya: la anomalía gravimétrica de la Laguna Merín. In: *15° Congreso Latinoamericano de Geología, 3° Congreso Uruguayo de Geología*. Actas Digitales, Montevideo.

Rojas, A. (2007). *Moluscos de aguas cálidas del Cuaternario Marino del Uruguay* (Master thesis). PEDECIBA, Universidad de la República.

Rosa, M. L., Tomazelli, L. J., Uberti, A. F., & Guimarães, E. (2009). Integração de métodos potenciais (gravimetria e magnetometria) na caracterização do embasamento da região sudoeste da bacia de pelotas, Sul do Brasil. *Brazilian Journal of Geophysics 27*(4), 1-18. https://doi.org/10.1590/S0102-261X2009000400008

Rossello, E., de Santa Ana, H., & Veroslavsky, G. (1999). El lineamiento Santa Lucía Aiguá Merín (Uruguay): Un rifting transtensivo Mesozoico abortado durante la apertura atlántica? In: *V Simposio sobre o Cretáceo do Brasil - I Simposio sobre el Cretácico de América del Sur*, Serra Negra, Brasil, pp. 443-448.

Rossello, E., de Santa Ana, H., & Veroslavsky, G. (2000). El Lineamiento Santa Lucía-Aiguá - Merín (Uruguay): Un corredor tectónico extensivo y transcurrente dextral precursor de la apertura Atlántica. *Revista Brasileira de Geociências*, *30*(4), 749-756.

Saadi, A. (1993). Neotectônica da Plataforma Brasileira: esboço e interpretações preliminares. *Geonomos*, *1*(1-2), 1-15. https://doi.org/10.18285/geonomos.v1i1e2.233

Saadi, A., Machette, M. N., Haller, K. M., Dart, R. L., Bradley, L. A., & Souza, A. M. P. D. (2002). *Map and database of quaternary faults and lineaments in Brazil*. International Lithosphere Program, Task Group II-2, Major Active Faults of the World. USGS/UFMG.

Sánchez-Bettucci, L., Cordani, U., Olivet, J., Peel, E., & Fort, S. (2021). The Nico Pérez Terrane and its Archean and Paleoproterozoic inheritance. *Andean Geology*, *48*(3), 442-471. https://doi.org/10.5027/andgeoV48n3-3345

Sanguinetti, Y. (1980). Bioestratigrafia (ostracodes) do Mioceno da Bacia de Pelotas, Rio Grande do Sul. *Pesquisas*, *13*(13), 7-34. https://doi.org/10.22456/1807-9806.21746

SESAME European Research Project (2004). *Guidelines for the implementation of the H/V spectral ratio technique on ambient vibrations - measurements, processing, and interpretations, deliverable D23.12*.

Soto, M., Morales, E., Veroslavsky, G., de Santa Ana, H., Ucha, N., & Rodríguez, P. (2011). The continental margin of Uruguay: Crustal architecture and segmentation. *Marine and Petroleum Geology*, *28*(9), 1676-1689. https://doi.org/10.1016/j.marpetgeo.2011.07.001

Sprechmann, P., Bossi, J., & Da Silva, J. (1981). Cuencas del Jurásico y Cretácico del Uruguay. In: Comité Sudamericano del Jurásico y Cretácico 1 (ed.), *Cuencas sedimentarias del Jurásico y Cretácico de América del Sur*. Comité Sudamericano del Jurásico y Cretácico 1.

Sprechmann, P., Ferrrando, L. A., & Martínez, S. (2000). Estado actual de los conocimientos sobre la Formación Camacho (Mioceno médio? – superior?, Uruguay). In: Aceñolaza, F. G., & Herbst, R. (eds.), *El Neógeno de Argentina* (v. 14, pp. 47-65). INSUGEO. Serie Correlación Geológica.

Tomazelli, L. J., & Villwock, J. A. (2000). O Cenozóico Costeiro do Rio Grande do Sul. In: Holz, M., & De Ros, L. F. (eds.), *Geologia do Rio Grande do Sul* (pp. 375-406). CIGO/UFRGS.

Ubilla, M. (2004). La Formación Fray Bentos (Oligoceno tardío) y los mamíferos más antiguos del Uruguay. In: Veroslavsky, G., Ubilla, M., & Martínez, S. (eds.), *Cuencas Sedimentarias del Uruguay. Geología, paleontología y recursos minerales. Cenozoico* (pp. 83-104). DIRAC, Facultad de Ciencias.

Ubilla, M., & Martínez, S. (2016). Geology and Paleontology of the Quaternary of Uruguay. *Springer Briefs in Earth System Sciences*. https://doi.org/10.1007/978-3-319-29303-5

Umpiérrez, R. (2022). *Caracterización de la cobertura sedimentaria del sector central de la Cuenca Laguna Merín (Uruguay) mediante el método HVSR* (Undergraduate thesis). Facultad de Ciencias, Universidad de la República.

Veroslavsky, G., de Santa Ana, H., & Rossello, E. (2004). Depósitos del Jurásico y Cretácico Temprano de la región meridional de Uruguay. El lineamiento Santa Lucía–Aiguá–Merín. In: Veroslavsky, G., Ubilla, M., & Martínez, S. (eds.), *Cuencas Sedimentarias del Uruguay. Geología, paleontología y recursos minerales. Mesozoico* 2. ed.pp. 117-134). DIRAC, Facultad de Ciencias.

Vieira, N. (1985). *Petrologia e geoquímica do vulcanismo mesozóico de Jaguarão, R.S., Brasil* (Master thesis). Universidade Federal de Rio Grande do Sul.

Vivanco, L., Morales, E., Caraballo, R., Oleaga, A., & Pacheco, C. (2020). Análisis magnetotelúrico del sector central de la Cuenca Laguna Merín, Uruguay. *Revista Investigaciones*, *3*, 1-13.